

Crystallization and multiple melting behavior of a new semicrystalline polyimide based on 1,3-bis(4-aminophenoxy)benzene (TPER) and 3,3',4,4'-biphenonetetracarboxylic dianhydride (BTDA)

V. Ratta, A. Ayambem, J.E. McGrath, G.L. Wilkes*

Department of Chemical Engineering, Department of Chemistry, NSF Science and Technology Center for High Performance Polymeric Adhesives and Composites, Virginia Tech, Blacksburg, VA 24061, USA

Received 17 May 2000; received in revised form 30 November 2000; accepted 30 November 2000

Abstract

This study introduces a novel high-temperature semicrystalline polyimide, which is based on an ether diamine (TPER or 1,3(4)APB) and BTDA dianhydride, both being commercially available. Phthalic anhydride is used as an endcap for improving thermal stability. The polyimide displays a T_g at ca. 230°C and two prominent melting endotherms at 360 and 416°C, respectively, with a sharp recrystallization exotherm following the lower melting endotherm. Significant recrystallization ability from the melt (at 450°C for 1 min) is observed with cooling rates faster than 200°C/min necessary to quench the polymer into an amorphous state. The effect of small variations in the melt crystallization temperature on the morphology and the melting behavior is discussed. DSC, hot stage polarized optical microscopy and WAXD experiments are utilized to interpret the melting behavior with respect to different causes. Some indirect evidence suggests that the two prominent melting endotherms may be due to different crystal unit cell structures. For crystallization temperatures higher than 350°C, an isothermal lamellar thickening phenomenon occurs with significant increases in the peak melting point (10–14°C) observed for longer crystallization times. © 2001 Elsevier Science Ltd. All rights reserved.

Keywords: Semicrystalline polyimide; Melting behavior; Thermal stability

1. Introduction

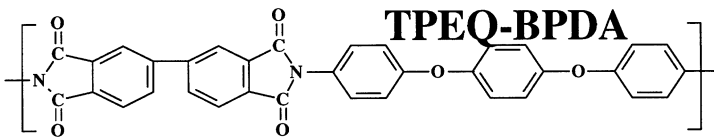
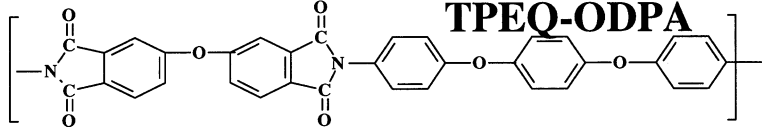
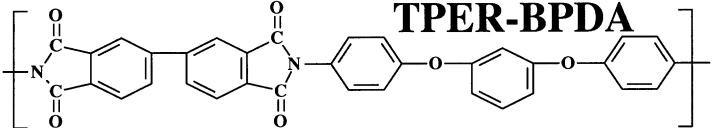
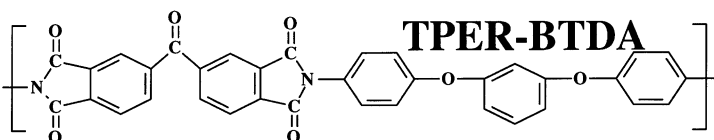
Polyimides are a class of thermally stable high-performance polymers that continue to gain importance in a wide variety of applications like high-temperature adhesives and composites, microelectronics, membranes and as photosensitive materials [1–3]. These applications are due to many desirable characteristics generally exhibited by polyimides including excellent mechanical properties, good radiation and chemical resistance, good adhesion properties and low dielectric constant. Presence of crystallinity in these materials can further substantially improve the thermal stability [4–6], solvent resistance [7], radiation resistance [8] and partial retention of mechanical properties above the T_g . In fact, one such polyimide, N-TPI (new thermoplastic poly-imide) has now been commercialized. In this regard, while many polyimides have been reported to exhibit crystallinity [9,10], most do not recrystallize once taken to the melt [4–6,11]. The initial crystallinity is, in

large part, due to the solvent-aided crystallization, which usually accompanies the imidization process, while the usually displayed slow crystallization kinetics limits the molecularly symmetric polyimide from crystallizing from the melt in reasonable time scales. Among the few polyimides that do show some evidence of crystallization from the melt, the recrystallization ability decreases rapidly with increasing times and temperatures in the melt. The T_g of these high-temperature polymers is usually in excess of 200°C and the melting points in the range of 400°C. The melt processing temperatures can thus often exceed 400°C and the poor melt recrystallization behavior thus, in part, can be explained due to the degradation reactions that can occur at these high temperatures. It is thus no surprise that polyimides are almost exclusively processed by a solvent route, which necessitates use of toxic solvents such as *N*-methyl pyrrolidinone (NMP), *N,N*-dimethyl formamide (DMF) and dimethyl acetamide (DMAc) among others. Additionally, these solvent-aided processes are more time consuming and expensive than the traditional melt-processing operations. It is thus obvious that development of melt-processable thermoplastic polyimides can be

* Corresponding author. Tel.: +1-540-231-5498; fax: +1-540-231-9511.
E-mail address: gwilkes@vt.edu (G.L. Wilkes).

Table 1

Previously developed high-temperature semicrystalline polyimides developed in our laboratories. Notice the high molecular weights of the repeat unit for each of these polyimides

	Repeat unit MW (Da)	T_g (°C)	T_m (°C)
 <p style="text-align: center;">TPEQ-BPDA</p>	550	259	471
 <p style="text-align: center;">TPEQ-ODPA</p>	550	238	420
 <p style="text-align: center;">TPER-BPDA</p>	566	210	395
 <p style="text-align: center;">TPER-BTDA</p>	578	230	416

beneficial from both an environmental and processing standpoint. With this in mind, several semicrystalline polyimides have been synthesized and characterized in our laboratories [4–6,11], some of which are shown in Table 1. Additionally, all these polyimides are based on commonly available dianhydrides and ether diamines and thus no separate step is required to prepare the monomers. Each of these polyimides shows crystallinity in the initial material, a high T_g and a high T_m . However, depending upon small differences in their structure, the success in terms of their melt crystallization behavior varies. Incorporating flexible ether or carbonyl linkages in the dianhydride and changing the nature of isomeric attachment in the diamines influences the melt crystallization behavior significantly. In an earlier work, we have shown that TPEQ–ODPA displays limited recrystallizability from the melt [12]. We found that the polyimide TPEQ–BPDA demonstrated a DSC peak melting point of 471°C and did not recrystallize once taken to the melt [11]. The third polyimide TPER or 1,3(4)APB (1,3-bis(4-aminophenoxy)benzene)–BPDA, however, has provided excellent results

from the melt recrystallization viewpoint. Our earlier works have shown the excellent thermal stability and melting characteristics [4–6], crystallization and morphological behavior [4,5], fast crystallization kinetics [6], rheological behavior [6] and very promising adhesive strengths and durability of this polyimide [4]. The work reported in this paper introduces another new semicrystalline polyimide (polyimide (d) in Table 1) based on 1,3-bis(4-aminophenoxy)benzene (TPER or 1,3(4) APB) and 3,3',4,4'-biphenonetetracarboxylic dianhydride (BTDA). The polyimide henceforth referred to as TPER–BTDA displays a T_g of ca. 230°C and two prominent melting endotherms with peak melting points of ca. 350 and 410°C. Additionally, the polyimide chains are endcapped with phthalic anhydride that serves to control the molecular weight and tremendously improves the thermal stability of the polyimide.

Several reasons for synthesizing the present polyimide exist. Traditionally BTDA-based polyimides have been found to be promising with respect to crystallization behavior [13]. An earlier study seemed to indicate that this material might be suitable from the melt recrystallization

standpoint [13]. Changing the dianhydride structure to BTDA also helps in better understanding of the structure property behavior in these ether diamine-based semicrystalline polyimides, due to a different chemical structure of the BTDA polyimide. Additionally BTDA-based polyimides are more attractive from a commercial viewpoint due to the lower cost of BTDA vis-a-vis most other dianhydrides.

The DSC melting behavior of this polyimide is interesting in that it demonstrates two distinct melting endotherms at ca. 350 and at ca. 410°C. As will be shown, additional endotherms develop depending upon the temperatures at which the polymer is crystallized. It is very important from both a fundamental and practical standpoint to understand the causes of this multiple melting behavior and how it may depend upon the previous thermal history. While such widely spaced distinct melting endotherms with a prominent intermediate crystallization exotherm have not commonly been observed, the problem of multiple melting behavior in semicrystalline polymers itself is not new. Multiple melting behavior has been observed in polyethylene [14–17], polypropylene [18–20], poly(ethylene terephthalate) (PET) [21–27], poly(butylene terephthalate) (PBT) [28–33], poly(phenylene sulfide) [34,35], poly(ether ether ketone) (PEEK) [36–55] semicrystalline polyimides [5,56–61] and other polymers. The multiple melting behavior can occur due to a variety of reasons like different crystal unit cell structures, presence of two or more distinct morphological forms or due to a continuous melting and recrystallization process. Other reasons presented in the literature include molecular weight fractionation [17], dependence on the heating rate in the DSC [62] and ascribing the lower endotherm to some sort of a physical aging process [45–47].

This study addresses the crystallization and multiple melting behavior of this polyimide by using the techniques of DSC, optical microscopy and WAXD. We will first introduce the polyimide by showing some evidence concerning the thermal stability and recrystallization ability from the melt. Thereafter, the effects of T_c (from the melt) on the melting behavior are discussed. Regarding the estimation of kinetics of crystallization, while the detailed quantitative methods like an Avrami analysis are not utilized in this study, some qualitative arguments are made on the basis of the observed results. Reasons for the multiple melting behavior and how this behavior may depend upon the previous T_c are explained on the basis of the evidence obtained. In this regard, experimental evidence is discussed in order to explain the multiple melting behavior on the basis of different crystal unit cell structures, the melting and recrystallization model and the morphological model. Results of the DSC experiments are shown for the isothermal crystallization for varying times at selected T_c s. The effect of heating rate on the melting behavior when crystallized at these temperatures is discussed. Lastly, some results are presented regarding the isothermal lamellar thickening phenomenon at relatively higher T_c s.

2. Experimental

2.1. Synthesis

1,3-Bis(4-aminophenoxy)benzene (TPER diamine) was supplied by Ken-Seika and was recrystallized from toluene before use. 3,3',4,4'-Biphenonetetracarboxylic dianhydride (BTDA) was supplied by the Occidental Chemical Corporation and was dried at 120°C prior to use. The endcapper phthalic anhydride (PA) was obtained from Aldrich and sublimed prior to use. *N*-methylpyrrolidinone (NMP) was obtained from Fisher and vacuum distilled after drying over P_2O_5 before use. The Carothers equation was utilized to calculate the monomer and endcapper concentration for synthesizing the desired M_n of 30,000 (30k) Da. The reaction vessel was a three-neck round bottom flask equipped with a mechanical stirrer, nitrogen inlet and a drying tube. Sufficient NMP was added to achieve a 10% solids concentration and the solution was allowed to stir for 24 h, to afford a homogenous poly(amic acid) solution as shown in Fig. 1. A stepwise thermal imidization procedure was utilized, which we have used successfully in the past. The first step was the casting of the poly(amic acid) precursor on the pyrex glass plates. These plates were placed in the vacuum oven overnight until smooth non-tacky films were obtained. Thermal imidization was achieved by raising the temperature to 100, 200 and 300°C and holding at each of these temperatures for 1 h. The time to go from one temperature to the next was ca. 1 h each at the fastest heating rate available with the oven. After the completion of the cycle, the plates were allowed to cool to room temperature before being removed from the oven. The films were stripped off the glass plates in hot water and stored in a dessicator before use.

2.2. Characterization

TGA studies utilized a Seiko TG/DTA and all experiments were carried in either a nitrogen or air atmosphere. The temperature was calibrated using indium and zinc standards and the dynamic experiments utilized a heating rate of

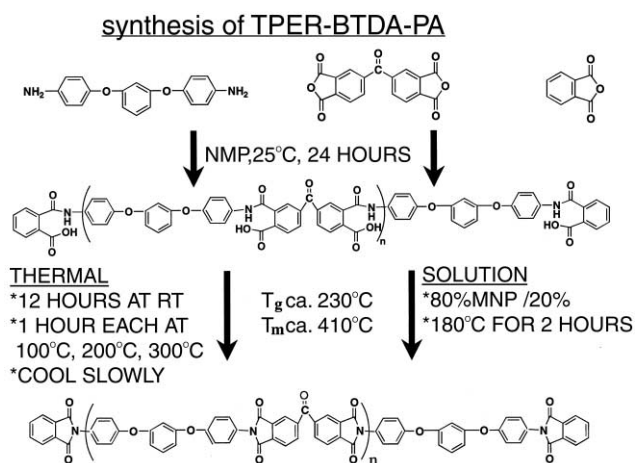


Fig. 1. Scheme for synthesis of TPER–BTDA–PA polyimide.

5°C/min. The isothermal experiments were performed for a duration of 180 min.

DSC experiments for both isothermal and non-isothermal crystallization were performed on a Perkin Elmer DSC-7. The amount of polymer utilized in a given thermal scan was kept between 6 and 8 mg. The DSC was calibrated with indium and zinc standards at the heating rate utilized. All experiments were conducted under a nitrogen purge and a DSC baseline was determined by running empty pans. For isothermal crystallization experiments, the samples were kept at room temperature and purged with nitrogen for 5 min to remove air from the DSC cell. The samples were then rapidly heated to 450°C for 1 min and cooling to below the T_g was done at the desired cooling rate or to the specific T_c s at 300°C/min. In this regard, data collection at high supercoolings was hampered by the initial instability of the DSC signal. This initial instability occurs on cooling to the T_c at fast cooling rates and may persist for ca. 1 min on our Perkin Elmer DSC 7. To perform a quantitative analysis like an Avrami analysis or to calculate the value of $t_{1/2}$ (time to attain 50% of the maximum crystallinity), some extrapolation of the initial portion of the exotherm is then usually undertaken (for the higher supercoolings), which promotes some degree of error in the final result. In this study, however, the peak time for the crystallization exotherm, t_p , for various T_c s only is reported. These values behave similarly as the quantitatively more precise $t_{1/2}$ and give a good indication of the crystallization kinetics at various supercoolings. For heating rates higher than 10°C/min, the sample

mass was reduced to 2–3 mg to minimize the thermal lag that may result at higher heating rates. All experiments were performed twice in order to maintain accuracy in the results. All reported DSC scans are normalized with respect to the sample mass (to 1 mg).

Polarized optical microscopy was carried out on a Zeiss optical microscope equipped with a Linkam 600 hot stage and 35 mm camera. The hot stage was calibrated using indium, tin and zinc. The film (~2 mils) was sandwiched between two glass slides and a nitrogen purge was maintained inside the hot stage. The sample was taken to 450°C and kept there for 1 min before being quenched to 340°C, kept there for 20 min and then rapidly heated to and held at 370°C. The quenching to 340 from 450°C was achieved by using a separate nitrogen source.

For WAXD experiments, a Siemens diffractometer equipped with a STOE Bragg–Brentano type goniometer and a wavelength of 1.54 Å was used after monochromatization through a graphite monochromator. Data was collected during a continuous scan at a speed of 0.5°/min between the angles of 10 and 60°.

3. Results and discussion

3.1. Thermogravimetric analysis

TGA was utilized to determine the material's thermal

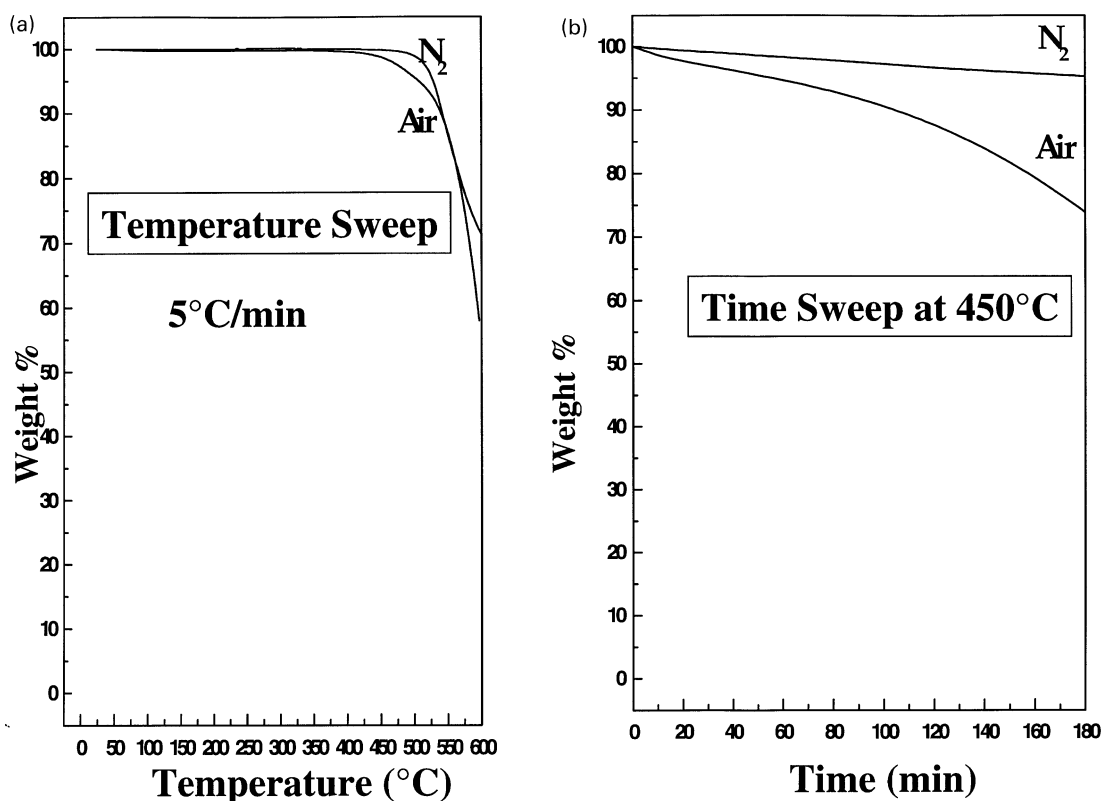


Fig. 2. (a) Dynamic heating profiles for weight loss in air and nitrogen when heated at 5°C/min. (b) Weight loss profile with time in air and nitrogen when kept at a typical melt temperature of 450°C.

stability as indicated by weight loss at higher temperatures. Dynamic experiments at a slow heating rate of 5°C/min were conducted from room temperature to 600°C in both air and nitrogen environments (Fig. 2(a)). The 5% weight loss temperatures in air and nitrogen are 507 and 529°C, respectively. As expected, the polymer exhibits significantly higher stability in nitrogen than in air, as the onset of weight loss appears to start in air at lower temperatures. These high weight loss temperatures are not surprising and are usually obtained for such polyimides. However, before comparing the values of these degradation temperatures with other studies, it needs to be remembered that faster rates will lead to even higher degradation temperatures because the polymer spends less time at any higher temperature.

While the degradation temperatures obtained in our case (at 5°C/min) are higher than the possible melt processing temperatures of ca 450°C, it is important to understand the effect of prolonged exposure at melt processing temperatures. In this regard, the isothermal scans for weight loss vs residence time in the melt, at a typical melt temperature of 450°C are shown for both in air and nitrogen (Fig. 2(b)). While the weight loss begins to occur in air for low-residence times, the polyimide shows very little weight loss even after 180 min in the melt at 450°C. The 5% weight loss times in air is 56 min, while 4.7% weight loss occurs in 180 min in nitrogen.

While the above traditionally utilized TGA experiments reveal the significant bulk thermal stability with respect to weight loss for this polyimide, no major inference can be made regarding the recrystallizability of the material from these temperatures. While TGA would detect the weight loss due to degradation reactions that are accompanied by emission of volatiles, other less severe reactions like crosslinking or chain branching may take place with little or no emission of volatiles, and thus little observable weight loss. These reactions, however, may significantly inhibit the ability of the material to crystallize from the melt. The increased viscosity that may result due to these reactions would also make the melt processing of the polymer difficult. Hence, TGA experiments, while serving as a gross measure of thermal stability, are of limited utility from understanding the stability from a recrystallization viewpoint. In this regard, DSC analysis to understand the crystallization from such high-melt temperatures is more appropriate.

3.2. Melting behavior

To understand the initial melting behavior and recrystallization response once heated above the T_m , DSC experiments were conducted by heating the polymer to a melt temperature of 450°C for 1 min and cooling at 300°C/min to below the T_g . Four consecutive scans are shown in Fig. 3. The initial material, which is crystalline, shows

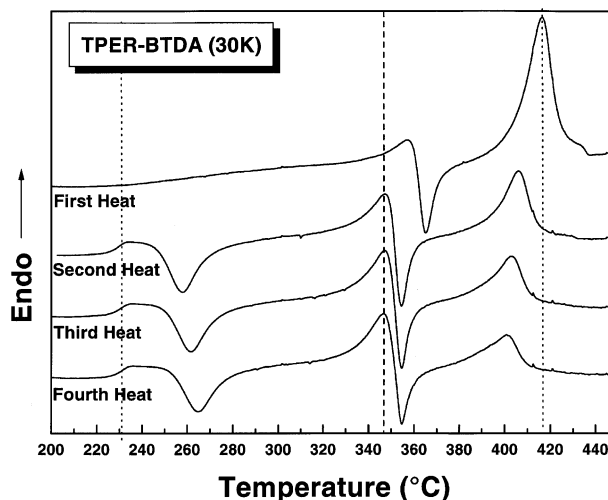


Fig. 3. Consecutive DSC heating scans after heating to 450°C at 10°C/min, holding for 1 min, quenching to 100°C and reheating at 10°C/min.

only a weak and broad T_g in the vicinity of 230–260°C. However, very interestingly, two prominent and widely spaced melting endotherms, with peak temperatures of 357 and 416°C, respectively, are observed. The first melting endotherm is rapidly followed by a recrystallization exotherm, which lies between the two melting endotherms. Such peculiar melting behavior is unusual for other semicrystalline polymers. It is noticed that in the initial material, the higher melting endotherm is significantly larger than the lower melting endotherm and the exotherm. In this regard, several features are observed, mainly:

1. The T_g becomes clearer (in terms of a narrow well-defined heat capacity jump) occurring at 230°C and is maintained for all the consecutive scans.
2. A prominent crystallization exotherm ca. 20°C appears above T_g . The peak temperature of this exotherm shifts to slightly higher temperatures with consecutive scans. The relative magnitude, however, does not change greatly.
3. The peak of the lower melting endotherm shifts downward to 347°C and both this peak temperature and the relative magnitude of this lower endotherm are maintained for the consecutive scans.
4. The recrystallization exotherm continues to appear after the first endotherm and shifts slightly to higher temperatures accompanied with moderate decrease in size. The higher melting endotherm continues to decrease in size and shifts to lower temperatures with repeated heating.

For the consecutive heating scans, the total enthalpy change (as given by ‘area under the endotherms – area under the exotherms’) is close to zero, thus indicating

that it was possible to quench the polymer to nearly an amorphous state from the melt. The well-defined T_g thus results from the removal of the constraints that were provided by the crystallites in the initial material. *The polyimide though, did not lose its ability to rapidly crystallize as evidenced by the crystallization exotherm just above the T_g .* However, the shift of this exotherm to higher temperatures with successive scans indicates that more thermal energy is required to induce crystallization. This is likely, in part, the result of a small amount of crosslinking/chain branching reactions that may occur each time the polyimide is heated to 450°C for 1 min. Such short time exposures, though, do not result in any observable weight loss, as already discussed previously. If any large-scale crosslinking reactions had occurred than the polyimide's ability to crystallize would be severely hampered, resulting in little or no crystallization during the heating scan. All experiments discussed henceforth in this publication only utilized melt conditions of 450°C for 1 min.

The construction of a baseline extending from just above the T_g to the end of the melting enables the calculation of the relative amount of crystal content associated with the respective crystallization exotherms and the melting endotherms. However, exact values are not reported here as results depend on slight variations in the placement of the baseline (due to the nature of the DSC curves). Nonetheless, some characteristics of the melting behavior are evident. Both the higher and lower melting forms are present in the initial material as the heat of fusion associated with the higher temperature peak is greater than the heat of crystallization of the intermediate exotherm. However, for the later scans, these amounts are nearly equal indicating that the higher melting form is primarily the result of recrystallization occurring after the lower melting endotherm. The lower melting form mainly is the result of melting of the crystals formed above T_g . While this melting response is obtained after quenching from the melt, it is also important to understand the effect of varying cooling rates on subsequent melting behavior. Studying the effect of cooling rate yields information on the crystallization kinetics. Fig. 4 shows the heating scans after the polyimide was cooled from the melt at different rates. Decreased cooling rates give the polyimide more time to crystallize during the cooling scan. This is clear from the T_g behavior and the crystallization behavior after the T_g . The heat capacity jump at T_g becomes relatively smaller and the magnitude of the crystallization exotherm after the T_g decreases tremendously as the cooling rate is decreased and the polyimide given enough time to crystallize. Interestingly though, the nature of the lower melting endotherm does not appear to change much. *It is interesting to observe that the higher melting crystals always form during the prominent recrystallization process during the heating process and not during the cooling process (even when the cooling rate is slow).* The adjacency of the intermediate crystallization

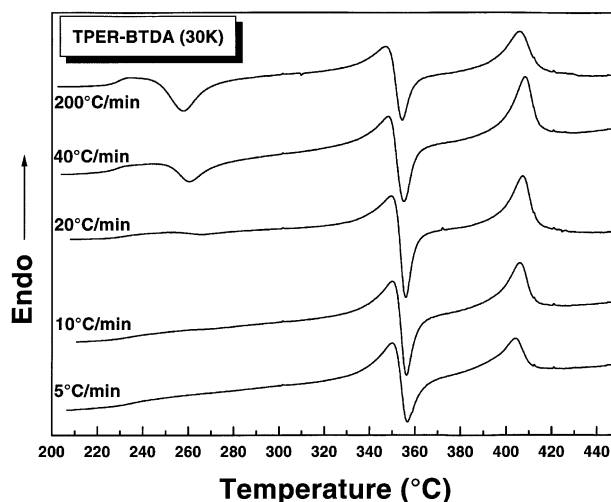


Fig. 4. Second heat DSC scans at 10°C/min after cooling from 450°C, 1 min at different cooling rates.

exotherm with the lower melting endotherm suggests that the crystallization is distinctly associated with melting of the previous crystals. One of the reasons for this could be that the fast recrystallization occurs at sites of just melted crystals. This proposal is further discussed in subsequent sections. Several reasons to elucidate the melting behavior can be offered, of which the three important ones are: (a) a continuous melting–recrystallization model to explain the lower melting endotherm and the higher melting endotherm; (b) a morphological model with the two endotherms representing melting of lamellae with different thickness, the thicker lamellae being formed due to the recrystallization at the higher T_c ; (c) different crystal unit cell structures being responsible for the two melting endotherms with the crystal transformation taking place during the recrystallization step.

3.3. Effect of crystallization temperature

Fig. 5(a) and (b) shows the heating scans after the polyimide was crystallized at temperatures ranging from 270 to 380°C after melt quenching from 450°C for 1 min. This range of T_c s covers the temperatures much below the position of lower endotherm, at the position of lower endotherm and recrystallization exotherm and also temperatures intermediate between the recrystallization exotherm and the higher melting endotherm. Fig. 5(a) shows the scans from room temperature after crystallizing at temperatures ranging from 270 to 330°C, all of which are below the position of the lower melting endotherm. The characteristic melting behavior of this polyimide with two widely spaced melting endotherms and an intervening recrystallization exotherm, are observed for all T_c s. A weak, third melting shoulder appears ca. 15°C above the previous T_c . It needs to be recognized that the position of the observed peak temperature

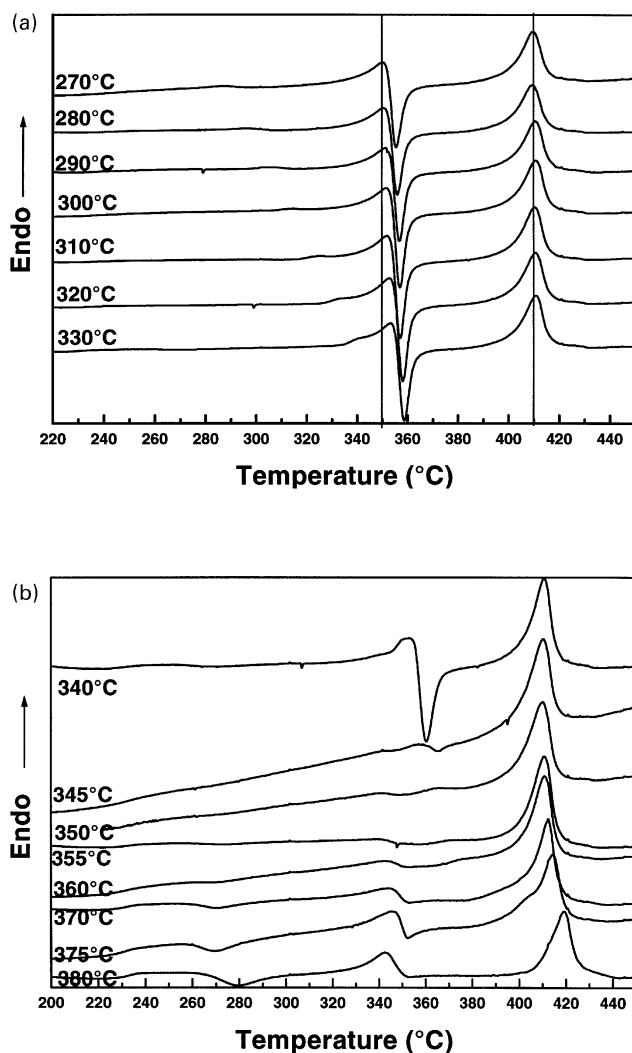


Fig. 5. (a, b) Scans from room temperature at 10°C/min after crystallizing at different temperatures from the melt at 450°C, 1 min.

for the lower melting endotherm may depend upon the subsequent recrystallization exotherm to some extent. This may occur due to the possibility of the recrystallization starting with the onset of the melting process. The DSC signal obtained in such a case then results from these two simultaneous processes. The shape of the melting and recrystallization behavior observed during the DSC scan thus depends upon the relative position of these two processes. In this regard, the recrystallization exotherm, which depends upon the melting of the crystals at ca. 350°C, shifts to higher temperatures with increasing T_c . The final endotherm, at ca. 410°C, is independent of the previous crystallization temperature for this range of T_c s.

Fig. 5(b) shows the heating scans after the samples were crystallized in the range 340–380°C. The lower melting shoulder that appears at ca. 15°C above the previous crystallization temperature occurs very close to the main lower melting endotherm for $T_c = 340^\circ\text{C}$, while the melting

behavior changes drastically as the T_c is raised just 5°C to 345°C. It is noticed that for sample crystallized at $T_c = 345^\circ\text{C}$, only a small endotherm at ca. 350°C is produced followed by immediate recrystallization and a final, larger melting endotherm at ca. 410°C. This indicates that at $T_c = 340^\circ\text{C}$, most of the crystals that form are those that melt at higher temperatures. The small population of lower melting crystals that result in the small endotherm at 350°C may form during the fast cooling to room temperature or during the heating scan from the room temperature. Similar behavior is obtained for T_c s greater than 350°C. In fact, for T_c greater than 360°C, a crystallization exotherm begins to appear during the heating scan resulting in formation of lower melting crystals. Also, the peak position of the higher melting endotherm begins to shift to higher temperatures as the T_c is increased to 380°C. For the T_c s above 350°C, the presence of any $T_c + 15^\circ\text{C}$ endotherm is difficult to detect. These results illustrate the significant effect that small changes in T_c can have on the melting behavior. The peculiar melting behavior, with two prominent endotherms, changes dramatically as the T_c is raised above 340°C. This has important ramifications from an application standpoint, where the polyimide may be used, for example, in high-temperature adhesive and composite applications. The modulus of the material is expected to show dramatic changes at ca. 350°C for the samples, which are crystallized below 345°C, while the modulus is expected to hold till much higher temperatures for samples crystallized above 340°C.

3.4. Crystallization kinetics

Another issue of significant importance is the crystallization kinetics at various isothermal temperatures. In this regard, the peak times for the isothermal crystallization exotherms are plotted in Fig. 6 and give a good indication

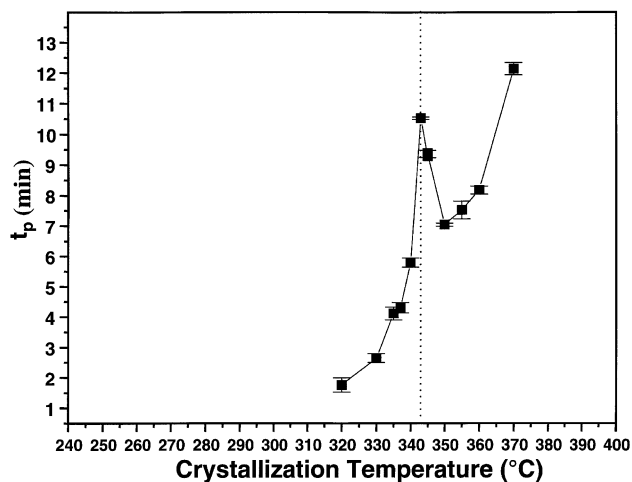


Fig. 6. Peak times for isothermal crystallization exotherms, after quenching from 450°C, 1 min to different crystallization temperatures. The error bars indicate the standard deviation of at least four samples.

of the kinetics of crystallization at various temperatures. The data was obtained by utilizing a minimum of four experiments for each T_c and the average values of peak times as well as the error bars indicating the standard deviation are plotted. It is a well-established fact that when the crystallization takes place in the nucleation-controlled region, the bulk crystallization rate increases as the degree of supercooling increases. In this regard, it is at first surprising to note the increase in peak crystallization times at intermediate T_c s with increasing ΔT . *This implies that the rate of crystallization starts to decrease with increasing supercooling in a narrow range of T_c s between 350 and 343°C!* These values of T_c s are close to the position of the lower melting endotherm. Also, as is previously discussed, the melting behavior of the polyimide changes dramatically when crystallized at T_c s above 340°C.

A conjecture for this peculiar behavior of crystallization half times is the presence of two crystal unit cell structures with different equilibrium melting points. While the formation of lower melting crystals is favored at temperatures below 345°C, higher T_c s promote the higher melting form. The rise in ‘peak crystallization times’ with increasing ΔT can then be explained due to slower crystallization rate of lower melting crystals being formed at these temperatures. This slower rate is due to (1) the lower ‘effective supercooling’ that is operative relative to the equilibrium melting point of these crystals and (2) the higher

melting crystals do not form below 350°C (unless solvent-induced crystallization occurs as in the initial material). As the T_c is lowered further, the supercooling increases again and crystallization rate increases. The peak crystallization times thus begin to decrease. During the heating scan, the lower melting crystals, if present, completely melt at temperatures in the vicinity of 345–350°C and subsequently give rise to the higher melting form. In this case, the size of the recrystallization exotherm depends upon the size of the previous melting endotherm. This evidence and the immediacy of the recrystallization then suggest that the recrystallization process is closely associated with the previous melting of the lower melting form. It is possible to contemplate that only a small conformational rearrangement is needed of the chains constituting the lower melting crystals to give rise to higher melting crystals. Additionally, as there is relatively little melt disorder, the nucleation density ‘in effect’ is very high for the subsequent crystals to grow. This would then explain the position and the fast rate of such a recrystallization process.

It is important to understand the morphological changes that might accompany this prominent bulk melting and recrystallization processes. To this end, a hot stage polarized optical microscopy experiment was conducted where the polyimide was rapidly quenched from the melt (450°C,

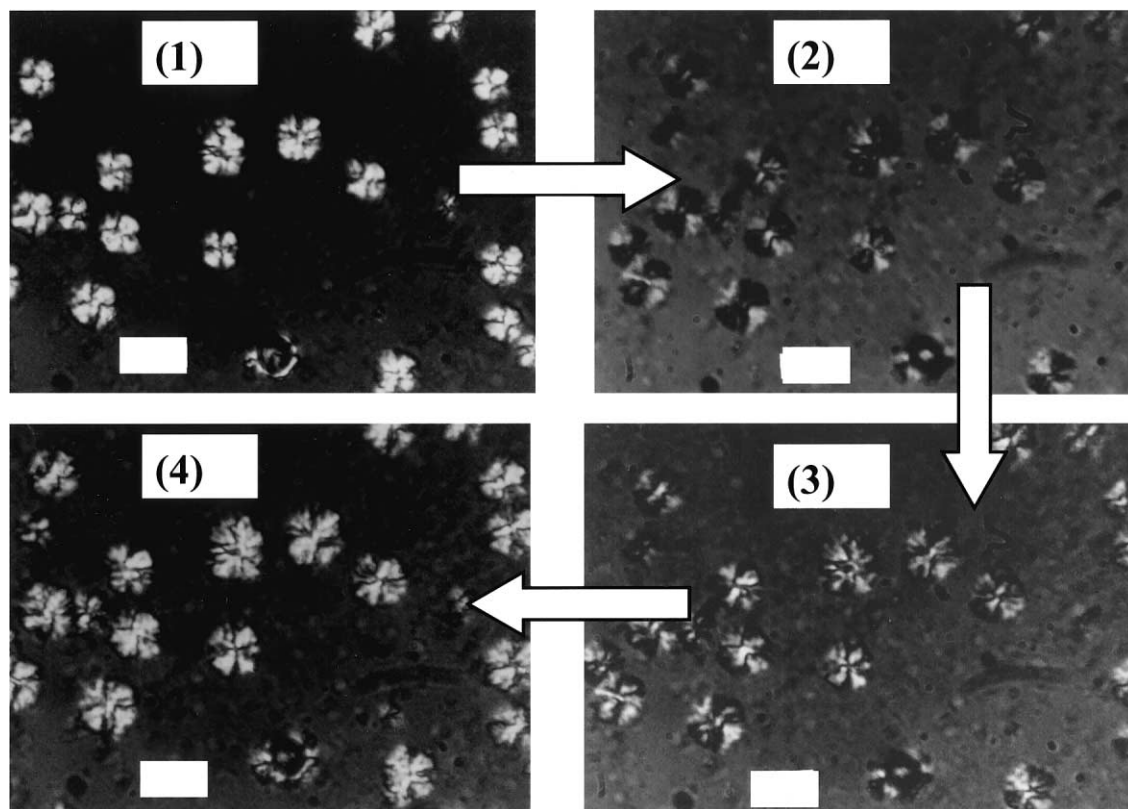


Fig. 7. Polarized optical micrographs of sample (1) crystallized at 340°C for 20 min and (2), (3), (4) held at 370°C for (1) 30 s, (2) 90 s and (3) 120 s. The error bars indicate 25 μm .

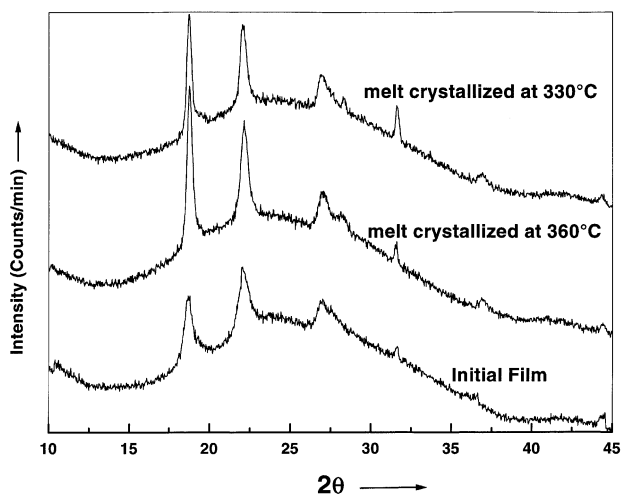


Fig. 8. WAXD patterns of TPER-BTDA-PA — initial film and melt crystallized at different temperatures. Samples were precisely prepared in the DSC.

1 min) to 340°C (where the low melting crystals form), crystallized at this temperature for 20 min and then *rapidly heated* to 370°C. Also, a more severe melt condition of 460°C for 3 min was utilized to reduce the residual nuclei in the melt and thereby reduce the nucleation density at 340°C, thus facilitating observation. A spherulitic morphology that appeared initially at 340°C, was then observed for any changes when the temperature was taken to 370°C. It was found that a very subtle and quick change occurred in the appearance of spherulites, when they were held at 370°C. This change is illustrated in Fig. 7, which illustrates the change in spherulitic morphology after the sample was

heated from 340 to 370°C. A coarse spherulitic morphology with only a weakly defined maltese cross is observed at 340°C. However, when heated to 370°C, these spherulites consisting of low melting crystalline form, melt and give rise to new spherulites at exactly the same position. The melting and recrystallization of the initial spherulites is illustrated in Fig. 7(2) and 7(3)), where the birefringence first changes on melting (compare Fig. 7(1) and 7(2)). However, following melting, immediate recrystallization leads to the re-emergence of spherulites that finally melt at ca. 410°C. If the temperature is held at 370°C, then the spherulites continue to grow at this temperature. In fact, from a polarized optical microscopy viewpoint, there is not much difference between the spherulites in Fig. 7(1) and 7(2), an observation also borne out by independent experiments at these two temperatures. This evidence explains to a large extent the reason for a sharp and adjacent recrystallization exotherm immediately after the lower melting endotherm. It also supports the earlier proposal of recrystallization occurring at about the same sites with a possible conformational rearrangement of the chains to give rise to a different crystal unit cell structure.

Subsequently, WAXD experiments were performed on samples crystallized above and below the temperature of the lower endotherm to verify if any noticeable difference in the X-ray patterns was obtained. The results obtained for the initial material and samples crystallized at 360 and 330°C are shown in Fig. 8. While the samples crystallized at 360 and 330°C are expected to, respectively, contain only the higher and lower melting crystalline forms, the DSC results indicate that the as-received initial polyimide contains both the higher and lower melting form. However, for the three different samples, no significant differences are

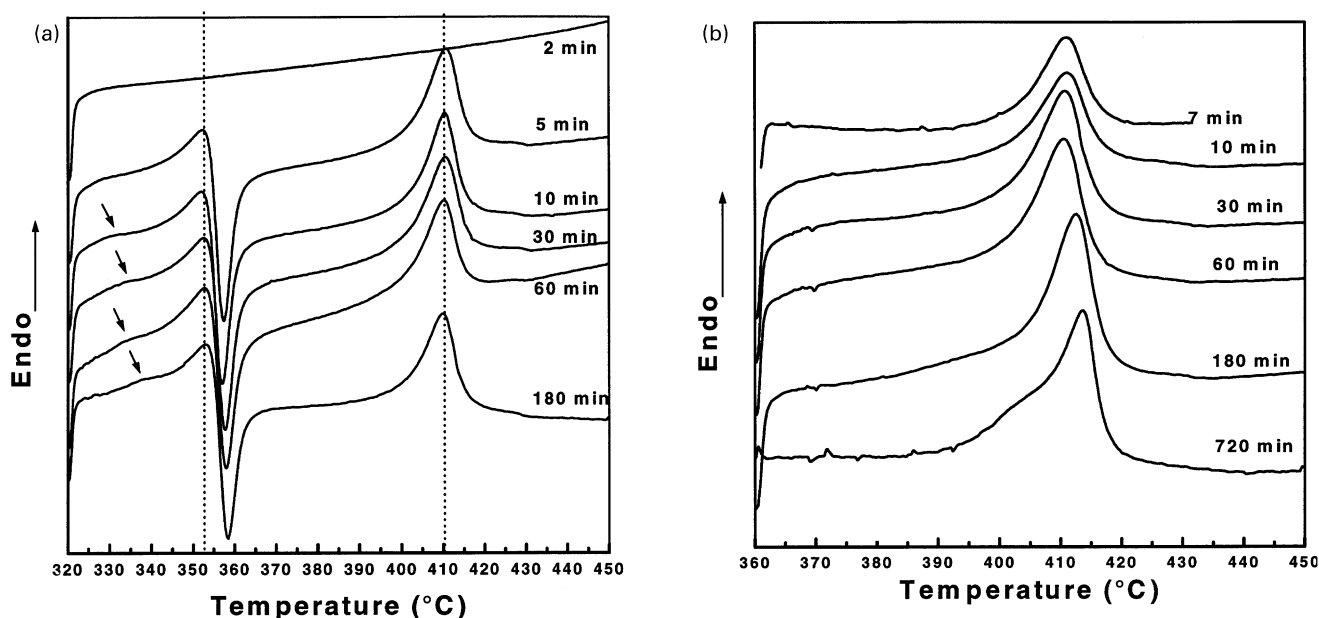


Fig. 9. Direct DSC heating scans at 10°C/min after crystallizing for various times at (a) 320 and (b) 360°C.

visible in terms of position of the peaks or presence of new ones. Our WAXD experiments are therefore not able to distinguish between the two different crystal unit cell structures (if they exist), which may be due to the close similarity between them. It has been shown that although PET (isotropic) shows two different crystal unit cells, only very sharply resolved WAXD experiments are able to resolve that difference. A more detailed information, possibly from a fiber pattern is required to resolve this difference. Thus in light of evidence demonstrated earlier, we contend that the presence of two prominent and widely spaced endotherms is the result of difference in crystal unit cell structures, though it did not lead to different WAXD results.

While we have ascribed two different crystal unit cell structures to be responsible for the two prominent endotherms, it remains unresolved whether the crystals undergo a continuous melting and recrystallization process before the melting endotherms appear or the melting endotherms represent the melting of crystals formed at the previous T_c . Further experiments were hence conducted to resolve this issue and correctly surmise the cause of the two melting endotherms. In this regard, two different types of experiments were conducted — one consisting of isothermal crystallization for varying times at the selected T_c and heating from that temperature and the other consisting of scans of previously crystallized specimens at varying heating rates. Also, two T_c s, 320°C (below the lower melting endotherm) and 360°C (between the two endotherms) were selected for this purpose. The results from the isothermal experiments are discussed first to see if convincing evidence supporting either of the two models is obtained.

Fig. 9(a) shows the direct heating scans from 320°C after the specimens were crystallized at that temperature for times indicated. Crystallinity appears in the specimens for higher residence times of 5–180 min. No major changes, however, are observed between different specimens with respect to the position and size of the two prominent endotherms and the intermediate recrystallization exotherm. Additionally, a small but noticeable endotherm (indicated by an arrow) appears ca. 10–15°C above 320°C for times greater than 5 min, with its strength showing a small increase and its position slightly shifting to higher temperatures for increasing crystallization times. This is followed by the primary lower melting endotherm, whose peak position or size does not change with increasing time. The result that the main melting endotherm at ca. 353°C appears first and the much weaker melting shoulder at ca. 330°C later, suggests that the primary and first forming crystals at $T_c = 320^\circ\text{C}$ are responsible for melting endotherm at ca. 353°C. The latter forming thinner crystals due to secondary crystallization are then responsible for the weaker lower melting shoulder.

For crystallization at 360°C, Fig. 9(b) shows the direct heating scans from 360°C after crystallizing for different times. In this case, no additional lower melting shoulder is observed, but rather only a broad melting endotherm at ca.

410°C is obtained. Also, for higher times of crystallization the amount of crystallinity continues to increase (as indicated by the size of the endotherm) while a shift in the position of peak melting point is also observed. No well-defined smaller endotherm ca. 10–15°C above the T_c is observed. The crystals melt over a broad range of temperatures starting from 370°C.

3.5. Effect of heating rate

To further substantiate the origin for the melting endotherms, experiments were conducted at varying heating rates for specimens originally crystallized at 320 and 360°C, respectively. Similar experiments were conducted on the original as-received polyimide film to detect any change in its melting behavior. Fig. 10(a) shows the DSC scans for the initial film heated at rates ranging from 5 to 150°C. The shape of the DSC scan for the different rates does not change much and consists of the characteristic prominent dual endotherms and an intermediate recrystallization exotherm. It is important to note, however, that the position of the lower melting peak does not change with heating rate. If this peak was the result of a continuous melting-recrystallization of previous crystals than the position of this peak is expected to shift to lower temperatures for faster heating rates, as lesser time is now available for the crystals to reorganize. Similar arguments can be extended for the behavior of the crystals associated with the higher melting peak, which does not show much change in its position. Also, both the recrystallization exotherm and higher melting endotherm broaden somewhat as the heating rate is increased. It is, however, interesting to note that recrystallization process is not greatly reduced even for significantly faster heating rates of 80 and 150°C/min, thereby indicating the extremely fast kinetics associated with this process. It is important to remember that the initial film undergoes a process of simultaneous chain extension/decyclohydration and solvent-aided crystallization during the imidization process leading to formation of higher and lower melting crystal forms.

Fig. 10(b) shows the DSC scans at different heating rates for film melt crystallized at 320°C for 1 h — the T_c where only the lower melting form is expected to form. Expectedly the melting behavior is quite different from the initial film. Whereas the lower melting peak shows a slight shift to higher temperatures for faster heating rates, the size and position of the higher melting form depends significantly on the heating rate utilized. In fact for the fastest heating rate of 150°C/min, the higher melting form is eliminated. This reduction in the higher melting form occurs concurrently with the reduction in the recrystallization process. Fig. 10(c) shows the DSC scans for polyimide-crystallized at 360°C for 1 h — a temperature where only the higher melting form is expected to form. The samples were quenched to room temperature before scanning at different rates. It is observed that while only one prominent

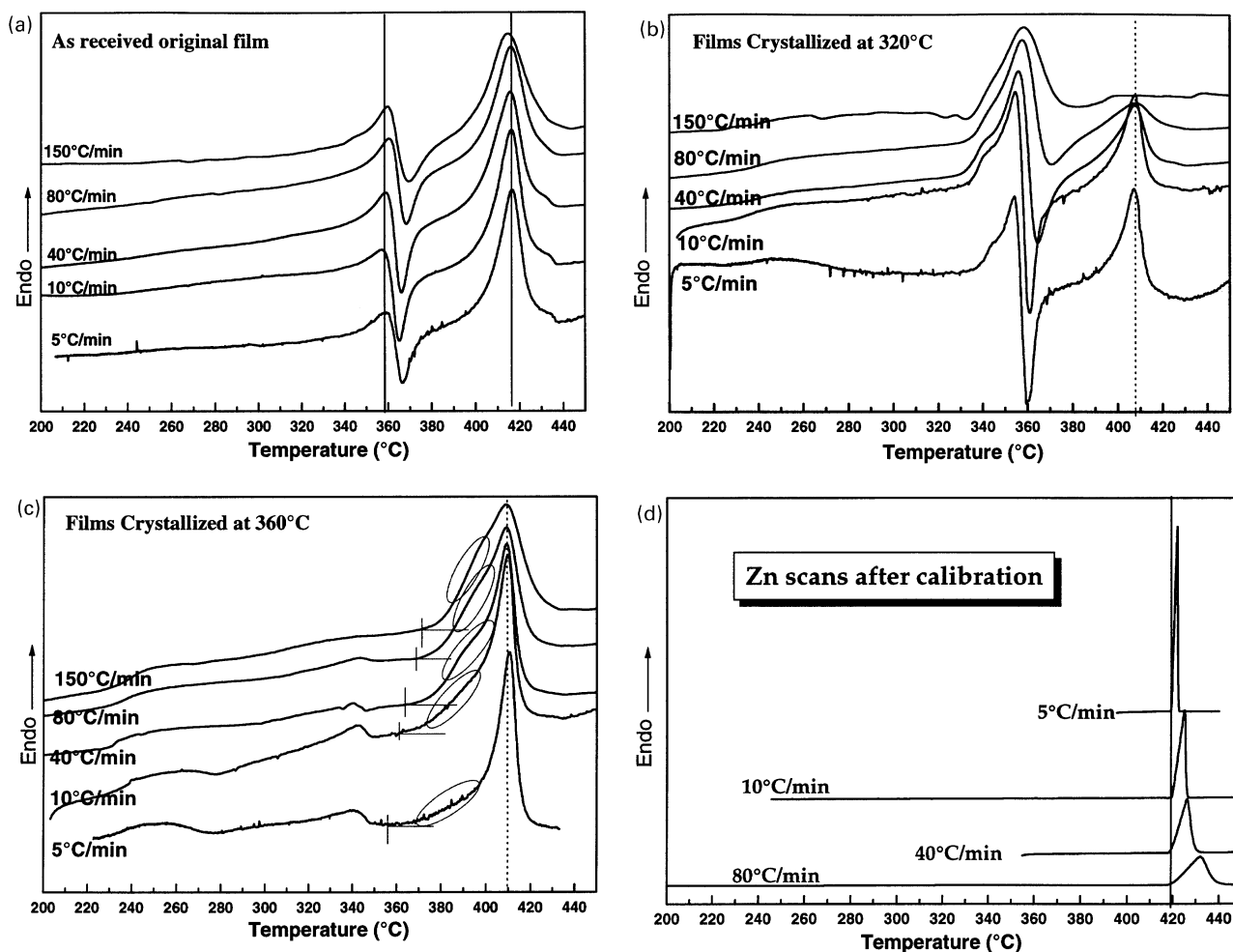


Fig. 10. DSC heating scans at different heating rates for: (a) initial film; (b) crystallized at 320°C; (c) crystallized at 360°C and (d) zinc after calibrating the DSC at different heating rates.

endotherm at ca. 410°C is observed, a smaller endotherm at ca. 340°C appears for slower heating rates. The appearance of the lower endotherm is due to the crystallization that occurs after the T_g . Faster heating rates reduce this crystallization thereby resulting in reduction of the melting endotherm at ca. 340°C. There is, however, no prominent recrystallization exotherm observed to give rise to higher melting crystals. It is useful to remember that this lower endotherm due to crystallization after T_g also occurred for T_c s greater than 360°C. This suggests that there may be a population of chains that more easily crystallize into the lower melting form, but require much longer times to crystallize into the higher melting form when at T_c s greater than ca. 360°C. The higher melting endotherm broadens considerably as the heating rate is increased, although there is no effect on the peak position. It is also noted that there is a low-temperature tail associated with the endotherm signifying the onset of melting of thinner crystals formed at 360°C. This melting starts after the temperature exceeds 360°C. The onset of melting seems to shift to slightly higher tempera-

tures for faster heating rates due to delayed melting. The effect of broadening of the various endotherms and exotherms observed in Fig. 10(a)–(c) is shown for the zinc specimens in Fig. 10(d) after calibrating at various heating rates. The onset of the melting point serves as a measure of the calibration and is obtained to within 0.3°C for various heating rates. However, the peak broadens for faster heating rates due to the thermal lag. Such an effect will be even more pronounced for the polymer samples. However, surprisingly, the position of the various peaks do not show any major shift to higher temperatures for faster rates.

3.6. Thickening of crystals

This polyimide demonstrates the commonly observed dependence of melting point on the previous T_c (see Fig. 5(b)). For temperatures above 350°C, it is observed that higher T_c s result in higher melting points. It is important to note here that there exists some difference in the higher

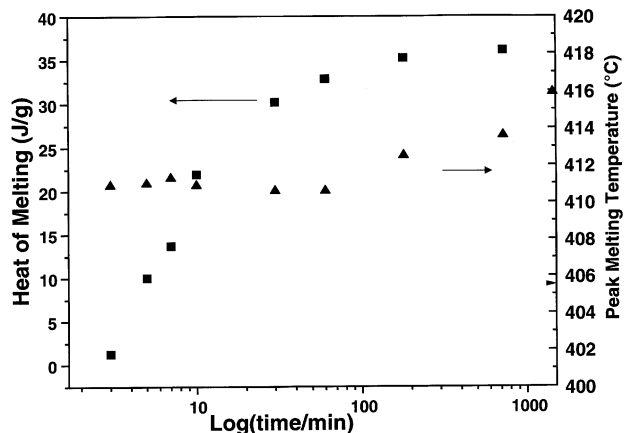


Fig. 11. Isothermal crystallization at 360°C with respect to logarithm of time. Squares refer to the heat of melting obtained after heating to melt.

melting point of the initial film and the films crystallized from the melt due to the solvent-induced crystallization being operative when imidization is taking place. It was shown earlier (Fig. 9(b)) that the melting point of the poly-

imide crystallized at 360°C shifts to higher temperatures for longer times of crystallization. The increases in T_m can occur due to isothermal or non-isothermal thickening of the original crystals formed at 360°C. To further investigate this phenomenon, detailed experiments were conducted at 360°C and higher temperatures for longer crystallization times (Figs. 11 and 12). The evolution of crystallinity was concurrently followed along with the variation in T_m as a function of time. Interestingly it was found that the T_m does not change much for residence times of ca. 100 min or less, while for longer crystallization times, a clear trend is observed in that T_m increases with the logarithm of crystallization time. In fact, significant increases of 10–14°C in the T_m were observed for higher T_c s and longer crystallization times. It is also noted that these increases in T_m are not accompanied by any sharpening/narrowing of the endotherms and thus cannot be solely attributed to crystal perfection or narrowing of the crystal thickness distribution. Rather the endotherms at higher temperatures are broader indicating a wider distribution of crystal thickness with time. This phenomenon, in our opinion, reflects the ‘crystal thickening’ effects occurring at longer crystallization times

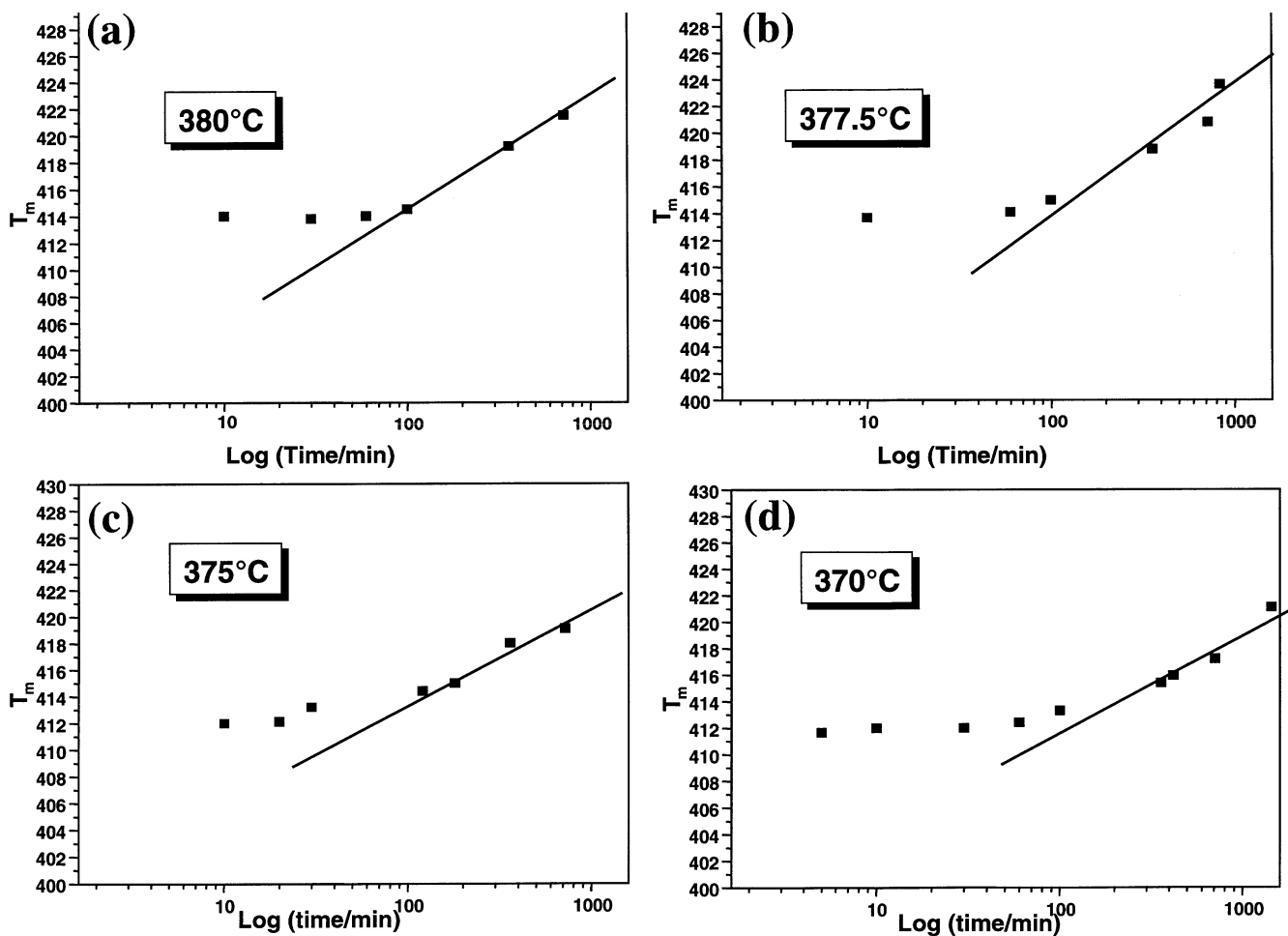


Fig. 12. Isothermal crystallization at various temperatures with respect to logarithm of time and the peak melting points obtained on heating for crystallization temperatures of: (a) 380, (b) 377.5, (c) 375, and (d) 370°C.

in the polyimide. There is an indication that the rate of thickening is faster for higher crystallization times, an observation commonly associated with such effects. However, it is peculiar to note that there seems to be an “onset time” associated with this process at 360°C. Fig. 11 shows the simultaneous evolution of crystallinity as indicated by heat of fusion. For shorter times, the faster increase is associated with the primary crystallization process, while for longer times, the heat of fusion begins to level off indicating the end of primary crystallization. It is important to note here that the onset of the thickening process is roughly associated with the ‘tapering off’ of the heat of fusion curve. The results therefore suggest that the thickening phenomena depend on the end of the primary crystallization. In this regard, it is relevant to first discuss the morphology of polyimide crystals. Our other studies using AFM and SAXS (data not shown) have indicated the presence of lamellar stacks within the material. However, the fold surfaces of these lamellae are not expected to be smooth. The long and semi-rigid nature of the chain will effectively block much adjacent or next neighbor reentry from taking place. It can therefore be conjectured that the nature of the fold surface is more akin to the switchboard model promulgated by Flory [63] and other workers [64]. While this model has remained controversial for polyolefins and other flexible polymers, it is more applicable for such rigid chain polymers as the one used in this study, which inherently cannot demonstrate a smooth and regularly folded surface due to their long and relatively more rigid chains. Thickening of the crystals then can only principally take place by the incorporation of the segments adjoining the ones already crystallized. At times shorter than needed for the primary crystallization to be over, the amount of such thickening (which it self depends on primary crystals) is expected to be small. This can then explain the absence of any noticeable crystal thickening effect for shorter times.

4. Conclusions

This work introduces a new thermally stable polyimide, which demonstrates a T_g of ca. 230°C and two distinct and widely spaced prominent endotherms at ca. 353 and 416°C. The polyimide exhibited significant recrystallization ability and moderately fast crystallization kinetics from the melt. The polyimide displays the usual increase in crystallization rate with increasing supercooling (i.e. in the nucleation-controlled regime) as evidenced by decreasing ‘peak’ crystallization times in the vicinity of 320°C. However, this trend is reversed in a narrow temperature range around 340–345°C, where the peak crystallization times showed an abrupt increase. The two main crystallization endotherms are conjectured to be due to difference in crystal unit cell structures. The lower melting crystals form below ca. 350°C while the higher melting crystals form at higher tempera-

tures. The abrupt increase in peak crystallization times (at ca. 340–345°C) is explained due to low supercooling experienced by the polymer at those temperatures with respect to the equilibrium melting point of the lower melting crystals.

Hot stage polarized optical microscopy reveals the presence of spherulitic morphology. It is observed that polyimide samples exhibiting spherulites at 340°C, when heated to 370°C, melt and rapidly give rise to the higher melting spherulites at exactly the same sites. This also explains the occurrence of fast recrystallization exotherm immediately proceeding the lower melting endotherm. It is proposed that only a small conformational rearrangement is needed of the chains constituting the lower melting crystals (once heated above their melting point), to give rise to the higher melting crystalline form. However, there does not seem to be a major difference in the crystalline structure as evidenced by our WAXD results.

The melting behavior depends significantly on the T_c , with an additional low melting shoulder appearing 10–15°C above the T_c when crystallized at temperatures below the position of the lower melting endotherm. When crystallized at these temperatures, the two prominent endotherms and an intermediate recrystallization exotherm are obtained. The melting behavior changes dramatically when crystallized at temperatures above 345°C. Only the higher melting crystals form at these temperatures leading to only one prominent melting endotherm at ca. 410°C.

An isothermal thickening phenomenon occurs at T_c s in excess of 350°C (giving rise to the higher melting crystals), as concluded from significant increases in T_{ms} (10–14°C) for samples crystallized for longer times. There, however, is an induction time for start of this thickening phenomenon, which corresponds roughly to the time needed for completion of the primary crystallization.

References

- [1] Hergenrother PM, Stenzenberger HD, Wilson D. Polyimides. London: Blackie, 1990.
- [2] Mittal KL, Ghosh MK. Polyimides, fundamentals and applications. New York: Marcel Dekker, 1996.
- [3] Polyimides: trends in materials and applications. In: Feger C, Khojasteh MM, Molis SE, editors. Proceedings of the Fifth International Conference on Polyimides. Ellenville, New York, Nov. 1994.
- [4] Ratta V, Stancik EJ, Ayambem A, Parvattareddy H, McGrath JE, Wilkes GL. Polymer 1999;40:1889.
- [5] Srinivas S, Caputo FE, Graham M, Gardner S, Davis RM, McGrath JE, Wilkes GL. Macromolecules 1997;30:1012.
- [6] Ratta V, Ayambem A, Young R, McGrath JE, Wilkes GL. Submitted for publication.
- [7] Chang AC, Hou TH, St. Clair TL. Polyimides: trends in materials and applications. In: Feger C, Khojasteh MM, Molis SE, editors. Proceedings of the Fifth International Conference on Polyimides. Ellenville, New York, Nov. 1994. p. 3.
- [8] Sasuga T. Polymer 1991;32:1012.
- [9] Tamai S, Yamaguchi A, Ohta M. Polymer 1996;37:3683.
- [10] Tamai S, Oikawa H, Ohta M, Yamaguchi A. Polymer 1998;39:1945.
- [11] Graham MJ, Srinivas S, Ayambem A, Ratta V, Wilkes GL, McGrath JE. Polym Prepr 1997;38(1):306.

- [12] Srinivas S, Graham M, Brink MH, Gardener S, Davis RM, McGrath JE, Wilkes GL. *Polym Engng Sci* 1996;36:1928.
- [13] Mitoh M, Asao K. *Polym Mater Encycl* 1996;8:6220.
- [14] Holden HW. *J Polym Sci* 1964;6:53.
- [15] Mandelkern L, Fatou JG, Denison R, Justin J. *J Polym Sci (B)* 1965;3:803.
- [16] Bair HE, Salovey R, Huseby TW. *Polymer* 1967;8:9.
- [17] Harland WG, Khadr MM, Peters RH. *Polymer* 1972;13:13.
- [18] Passingham C, Hendra PJ, Cudby MEA, Zichy Z, Weller M. *Eur Polym J* 1990;26(6):631.
- [19] Samuels RJ. *J Polym Sci (B)* 1975;13:1417.
- [20] Edwards BC. *J Polym Sci (B)* 1975;13:1387.
- [21] Groeninckx G, Reynaers H. *J Polym Sci (B)* 1980;18:1325.
- [22] Holdsworth PJ, Turner-Jones A. *Polymer* 1971;12:195.
- [23] Qiu G, Tang Z, Huang N, Gerking L. *J Appl Polym Sci* 1998;69:729.
- [24] Tan S, Su A, Li W, Zhou E. *Macromol Rapid Commun* 1998;19:11.
- [25] Woo EM, Ko TY. *Colloid Polym Sci* 1996;274:309.
- [26] Alfonso GC, Pedemonte E, Ponzetti L. *Polymer* 1979;20:105.
- [27] Zhou C, Clough SB. *Polym Engng Sci* 1988;28(2):65.
- [28] Stein RS, Misra RS. *J Polym Sci (B)* 1980;18:327.
- [29] Nichols ME, Robertson RE. *J Polym Sci (B)* 1992;30:755.
- [30] Cheng SZD, Pan R, Wunderlich B. *Makromol Chem* 1988;189:2443.
- [31] Yeh JT, Runt J. *J Polym Sci (B)* 1989;27:1543.
- [32] Kim HG, Robertson RE. *J Polym Sci (B)* 1998;36:1417.
- [33] Qudah AMA, Raheil AA. *Polym Int* 1995;38(4):375.
- [34] Chung JS, Cebe P. *Polymer* 1992;33(11):2312.
- [35] Chung JS, Cebe P. *Polymer* 1992;33(11):2325.
- [36] Lattimer MP, Hobbs JK, Hill MJ, Barham PJ. *Polymer* 1992;33:3971.
- [37] Lee Y, Porter RS, Lin JS. *Macromolecules* 1989;22:1756.
- [38] Lee Y, Porter RS. *Macromolecules* 1987;20:1336.
- [39] Jonas AM, Russell TP, Yoon DY. *Macromolecules* 1995;28:8491.
- [40] Blundell DJ. *Polymer* 1987;28:2248.
- [41] Blundell DJ, Osborn BN. *Polymer* 1983;24:953.
- [42] Cheng SZD, Cao MY, Wunderlich B. *Macromolecules* 1986;19:1868.
- [43] Verma RK, Velikov V, Kander RG, Marand H. *Polymer* 1996;37:5357.
- [44] Marand H, Prasad A. *Macromolecules* 1992;25:1731.
- [45] Marand H, Velikov V, Netopilik M. *Polym Prepr* 1993;34(2):239.
- [46] Marand H, Velikov V. *Polym Prepr* 1993;34(2):835.
- [47] Marand H, Velikov V. *J Therm Anal* 1997;49:375.
- [48] Verma R, Marand H, Hsiao B. *Macromolecules* 1996;29:7767.
- [49] Hsiao BS, Sauer BB, Verma R, Zachmann HG, Seifert S, Chu B, Harney P. *Macromolecules* 1995;28:6931.
- [50] Hsiao BS, Gardner KH, Wu DQ, Chu B. *Polymer* 1993;34:3986.
- [51] Hsiao BS, Gardner KH, Wu DQ, Chu B. *Polymer* 1993;34:3996.
- [52] Kumar S, Anderson DP, Adams WW. *Polymer* 1986;27:329.
- [53] Bassett DC, Olley RH, Raheil AMA. *Polymer* 1988;29:1745.
- [54] Kroger KN, Zachmann HG. *Macromolecules* 1993;26:5202.
- [55] Deslandes Y, Day M, Sabir NF, Suprunchuk T. *Polym Comp* 1989;10:360.
- [56] Brandom DK, Wilkes GL. *Polymer* 1995;36:4083.
- [57] Brandom DK, Wilkes GL. *Polymer* 1994;35:5672.
- [58] Kreuz JA, Hsiao BS, Renner CA, Goff DL. *Macromolecules* 1995;28:6926.
- [59] Hsiao BS, Kreuz JA, Cheng SZD. *Macromolecules* 1996;29:135.
- [60] Sauer BB, Hsiao BS. *Polymer* 1995;36:2553.
- [61] Hsiao BS, Sauer BB, Biswas A. *J Polym Phys* 1994;32:737.
- [62] Harrison IR. *Polymer* 1985;26:3.
- [63] Yoon DY, Flory PJ. *Faraday Discussions of the Chemical Society*, n68. *Organization of Macromolecules in the Condensed Phase*, 1979. p. 288.
- [64] Mandelkern L. *Characterization of materials in the research: ceramics and polymers*. Syracuse, New York: Syracuse University Press, 1975 (p. 369).